Padé and K-matrix approximations to the O($2N$) model for large N

Scott Willenbrock
Physics Department, Brookhaven National Laboratory, Upton, New York 11973
(Received 16 August 1990)

The Padé approximation and the K matrix are techniques for constructing perturbative amplitudes which satisfy two-body unitarity exactly. We apply these approximations to the Goldstone-boson scattering amplitude in a spontaneously broken O($2N$) model, in the large-N limit, and compare with the exact amplitude (to leading order in $1/N$). The $[r,r]$ Padé approximation reproduces the exact large-N amplitude for all r. The K matrix, at any finite order, yields an amplitude which is qualitatively similar to, but not identical to, the exact amplitude.

I. INTRODUCTION

In the absence of a "light" Higgs boson, the scattering of longitudinal weak vector bosons becomes strong in the TeV energy regime. This is reflected in the fact that the $I=0$, $J=0$ Born amplitude for longitudinal-vector-boson scattering violates the unitarity bound, for energies above the Higgs resonance, if $m_H \gtrsim 800$ GeV.[1] Similarly, if the Higgs boson is absent altogether, the unitarity bound is violated at the tree level in longitudinal-vector-boson scattering at energies in excess of about 1.2 TeV.[2,3]

If longitudinal vector bosons are strongly coupled in the TeV energy regime, the associated physics may be very rich. On the other hand, our ability to predict this physics is greatly impeded by the fact that the usual perturbative calculational techniques are not reliable. One approach to ameliorating this situation, which has been espoused by several authors,[4-9] is to extend the usual perturbative techniques such that two-body unitarity is exactly satisfied. Since two-body unitarity is a nonperturbative property of the S matrix (assuming multiparticle states may be neglected), the hope is that the unitarized perturbative approach will reflect some of the nonperturbative aspects of the theory. This approach has also been applied to pion physics.[10-13]

It is difficult to gauge the validity of the unitarized perturbative approach, which lies somewhere between a perturbative and nonperturbative technique. If we could solve the longitudinal-vector-boson system exactly, we could compare it with the results of the unitarized perturbative calculation to judge its accuracy. Of course, there would then be no need for the unitarized perturbative calculation. One may also adopt the point of view that the ultimate test of the validity of this approach lies with experiment. However, if nature does resemble the "predictions" of this approach, one cannot rule out the possibility that this resemblance is fortuitous.

Another method to study the validity of the unitarized perturbative approach is to apply it to systems which, although not necessarily of physical interest, can be solved exactly. The O($2N$) scalar field theory (with the scalar field in the fundamental representation) in the large-N limit is such a model; it can be solved "exactly" to leading order in $1/N$.[14-17] This model corresponds to the scalar sector of an SU(N) gauge theory, with the scalar field in the fundamental representation of SU(N). In the real world $N=2$, which is not a large number. However, we are not advocating the use of the large-N limit as a model of the real world, but are using it as a testing ground for unitarized perturbative techniques. Nevertheless, the motivation for choosing this model is that it is an extension of the scalar sector of the standard Higgs model.[16]

We assume that the symmetry of the O($2N$) scalar theory is spontaneously broken to O($2N-1$), producing $2N-1$ Goldstone bosons and a Higgs boson. In the gauged SU(N) model, the Goldstone bosons are absorbed (in unitary gauge) to produce $2N-1$ massive vector bosons. If we take the limit of vanishing gauge coupling, $g \to 0$, keeping the scalar-field vacuum expectation value v fixed, the $2N-1$ massive vector bosons become massless ($M_V \sim gv$). The Goldstone bosons (which are present in R_ξ gauge) then represent the longitudinal vector bosons, and the scalar sector decouples from the gauge sector. Therefore, the O($2N$) scalar model in the broken phase may be regarded as the $g \to 0$ limit of an interacting system of longitudinal vector bosons and a Higgs boson. The only interactions that survive in this limit are proportional to the scalar-field self-interaction, $\lambda \sim g^2 m_H^2/M_V^2 \sim m_H^2/v^2$.

In this paper we calculate the Goldstone-boson scattering amplitude in the O($2N$) model in the large-N limit using two well-known unitarization techniques: the Padé approximation[6-12] and the K matrix.[4-6,9,13] We compare the amplitudes with the exact amplitude, obtained by summing the diagrams which dominate in the large-N limit. The results of our investigation may be summarized as follows.

(1) The $[r,r]$ Padé approximation to the Goldstone-boson scattering amplitude is identical to the exact amplitude for all r.

(2) The tree-level K matrix yields an amplitude qualitatively similar to, but not identical to, the exact amplitude. The K-matrix amplitude differs from the exact amplitude at any finite order, approaching the exact amplitude at infinite order.

Sections II–IV are devoted to the O(2N) model, the Padé approximation, and the K matrix, respectively. Section V contains a discussion of our results. The analytic structure of the scattering amplitude is discussed in the Appendix.

II. THE O(2N) MODEL

The Lagrangian of the O(2N) model is

$$\mathcal{L}=\tfrac{1}{2}\partial_\mu\phi^a\partial^\mu\phi^a-\tfrac{1}{4}\lambda_0(\phi^a\phi^a-v^2)^2 , \tag{2.1}$$

where ϕ^a is a $2N$-component real scalar field, and a sum on repeated indices is implied. The potential is chosen such that the O(2N) symmetry is broken. As usual, we shift the last component of the field to the minimum of the potential, $\phi^{2N}\rightarrow H+v$. The Lagrangian becomes

$$\mathcal{L}=\frac{1}{2}\partial_\mu\phi^a\partial^\mu\phi^a+\frac{1}{2}\partial_\mu H\partial^\mu H -\frac{1}{8}\frac{m_0^2}{v^2}(\phi^a\phi^a+H^2+2Hv)^2 , \tag{2.2}$$

where a now runs up to $2N-1$ only. There are $2N-1$ massless Goldstone bosons and a Higgs boson with a bare mass squared of $m_0^2=2\lambda_0 v^2$.

The existence of a broken phase of the O(2N) model in the large N limit has a long history, beginning with the work of Coleman, Jackiw, and Politzer, who found a tachyon pole in the Higgs propagator and concluded that the broken phase is unstable.[14,15] Today it is widely believed that fundamental scalar field theories are trivial; i.e., the renormalized coupling vanishes as the cutoff is taken to infinity.[18] However, if we regard the scalar field theory as an effective field theory, valid up to some energy scale, Λ, at which it is presumably subsumed by some deeper theory, then a nontrivial renormalized coupling exists. Furthermore, the tachyonic pole occurs for $|p^2|\gtrsim\Lambda^2$, so it lies outside the region of validity of the theory, and may be ignored.[15,16]

The Goldstone-boson scattering amplitude in the O(2N) model, to leading order in $1/N$, but to all orders in $\lambda_0 N$, was first computed by Bardeen and Moshe.[15] It was later analyzed in detail by Einhorn,[16] who adopted the effective-field-theory point of view. We rederive the results of this investigation in order to compare them with the Padé approximation and K-matrix results. Since the Higgs boson is a singlet under the residual O($2N-1$) symmetry, it couples to the (normalized) state $[1/\sqrt{2(2N-1)}]|\phi^a\phi^a\rangle$ (sum on repeated indices implied). For convenience, we consider the elastic scattering amplitude of this state.

The dominant diagrams in the large N limit which contribute to $\phi^a\phi^a\rightarrow\phi^b\phi^b (a\neq b)$ are shown in Fig. 1. The singlet scattering amplitude at the tree level is

$$A_1=-N\frac{m_0^2}{v^2}\frac{s}{s-m_0^2} , \tag{2.3}$$

where we have dropped terms of order $1/N$ with respect to the leading term.[19] The second-order amplitude is

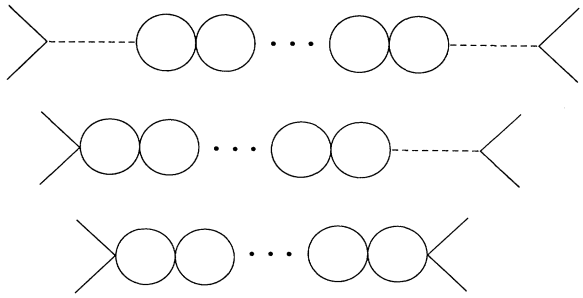

FIG. 1. Feynman diagrams which contribute to $\phi^a\phi^a\rightarrow\phi^b\phi^b$ ($a\neq b$) in the large-N limit.

$$A_2=(A_1)^2 I(s) , \tag{2.4}$$

where

$$I(p^2)=\int\frac{(d^{4-2\epsilon}k)_E}{(2\pi)^{4-2\epsilon}}\frac{1}{k^2(k+p)^2} =\frac{1}{(4\pi)^2}\left[\frac{1}{\epsilon}-\gamma+2-\ln\frac{-p^2}{4\pi\mu_0^2}\right] \tag{2.5}$$

is the loop integral associated with the bubble diagram (after Wick rotation), which we have evaluated in $4-2\epsilon$ dimensions to regulate the ultraviolet divergence. Since massless, quadratically divergent loop integrals vanish in dimensional regularization, the Higgs vacuum expectation value v remains unrenormalized, and we may ignore all tadpole diagrams.

The lth-order contribution to the singlet Goldstone-boson scattering amplitude is

$$A_l=(A_1)^l[I(s)]^{l-1} . \tag{2.6}$$

Summing the amplitude to all orders yields

$$A=\sum_{l=1}^{\infty}A_l=\frac{A_1}{1-A_1 I(s)} =-N\frac{m_0^2}{v^2}\frac{s}{s-m_0^2+Ns(m_0^2/v^2)I(s)} , \tag{2.7}$$

which is the singlet Goldstone-boson scattering amplitude in the large N limit. The zeroth partial wave of this amplitude, defined by

$$a=\frac{1}{32\pi}\int_{-1}^{1}dz\ A \tag{2.8}$$

(z is the cosine of the scattering angle), satisfies the two-body unitarity relation

$$\mathrm{Im}a=|a|^2 . \tag{2.9}$$

The divergence in the loop integral $I(s)$ may be absorbed into a scale-dependent renormalized mass parameter, defined by

$$m_R^2(\mu^2)=\frac{m_0^2}{1+N(m_0^2/v^2)\mathrm{Re}I(\mu^2)} , \tag{2.10}$$

which yields the renormalized amplitude

$$A=-N\frac{m_R^2}{v^2}\frac{s}{s-m_R^2-Ns[m_R^2/(4\pi v)^2]\ln(-s/\mu^2)}\ . \tag{2.11}$$

The renormalized mass parameter may be related to a renormalized coupling by $\lambda_R\equiv m_R^2/2v^2$.

The physical Higgs particle appears as a pole in the scattering amplitude on the second (unphysical) Riemann sheet. Einhorn[16] has shown how to find the position of the pole by making a judicious choice of the renormalization scale μ^2. Let the position of the pole be given by $s_0=\mu^2 e^{i\theta}$, i.e., choose $\mu^2=|s_0|$. The physical mass and width of the Higgs resonance, defined by

$$s_0=\left[m_H-\frac{i}{2}\Gamma_H\right]^2\ , \tag{2.12}$$

are then given by

$$m_H=\mu\cos\frac{\theta}{2}\ , \tag{2.13}$$

$$\Gamma_H=-2m_H\tan\frac{\theta}{2}\ , \tag{2.14}$$

where θ is determined via

$$\tan\theta=N\frac{m_R^2}{(4\pi v)^2}(\theta-\pi) \tag{2.15}$$

and μ^2 via

$$\mu^2=m_R^2\cos\theta\ . \tag{2.16}$$

For a given value of N and m_R^2, one solves Eq. (2.15) for θ, uses Eq. (2.16) to find μ^2, and then finds m_H and Γ_H via Eq. (2.13) and Eq. (2.14).

We discuss the analytic structure of the scattering amplitude, Eq. (2.11), in the Appendix. We show that there is a pole on the second Riemann sheet, below the real axis ($-\pi/2<\theta<0$), corresponding to the physical Higgs particle. We also show that there are no poles on the physical sheet, except a tachyon pole, which we will discuss shortly.

In order to demonstrate how the physical-Higgs-boson mass varies with m_R^2, we must choose some value for N/v^2. To make contact with the real world, we choose $v=246$ GeV and $N=\frac{3}{2}$. The latter choice is motivated by the observation that there are $2N-1$ Goldstone bosons which we have summed in the loops, but we have written N rather than $(2N-1)/2$ for simplicity (they are equivalent for large N). Thus, setting $N=\frac{3}{2}$ corresponds to an O(4) model, as desired.

Figure 2 shows the physical-Higgs-boson mass as a function of the renormalized mass parameter m_R. We find that as m_R approaches 1.4 TeV the physical-Higgs-boson mass saturates at 1 TeV. As we increase m_R beyond 1.4 TeV, the physical-Higgs-boson mass begins to decrease slowly, approaching 822 GeV as $m_R\to\infty$. However, the region $m_R\gg 1$ TeV may not be trustworthy, because the physical-Higgs-boson mass is comparable to the scale at which m_R blows up; presumably the effective-field-theory description breaks down prior to this energy. For a given $m_R(\mu^2)$, the scale Λ_0 at which m_R blows up may be obtained from the renormalization-group equation

$$\frac{1}{m_R^2(\mu^2)}=\frac{1}{m_R^2(\mu_0^2)}-\frac{N}{(4\pi v)^2}\ln\frac{\mu^2}{\mu_0^2}\ , \tag{2.17}$$

which may be derived from Eq. (2.10). Setting $m_R(\Lambda_0^2)=\infty$, we obtain

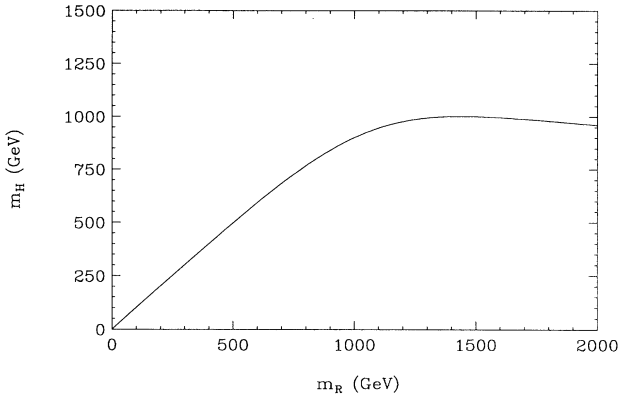

FIG. 2. The physical-Higgs-boson mass as a function of the renormalized mass parameter in the O(2N) model for large N. The physical mass goes to 822 GeV as $m_R\to\infty$.

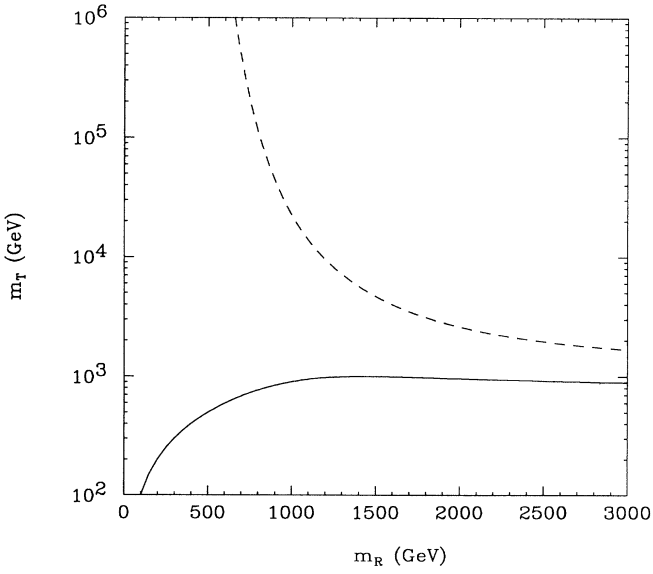

FIG. 3. The tachyon mass ($m_T^2=-s_0$, where s_0 is the tachyon pole) as a function of the renormalized mass parameter in the O(2N) model for large N (dashed). The physical-Higgs-boson mass is also shown (solid).

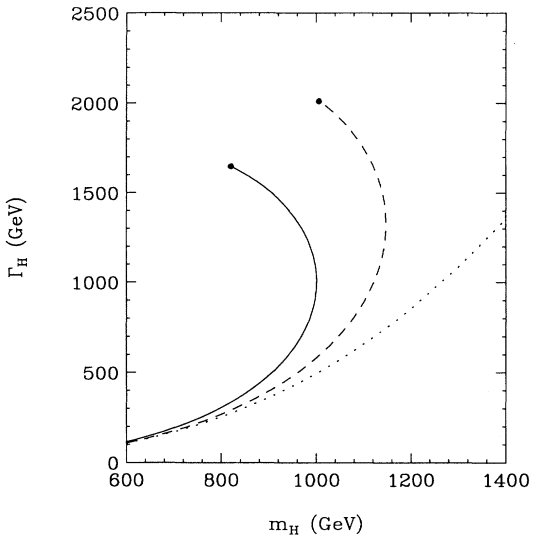

FIG. 4. The Higgs-boson width as a function of the physical-Higgs-boson mass in the O(2N) model for large N (solid) and in the tree-level K-matrix approximation (dashed). The tree-level perturbative estimate is also shown (dotted).

$$\Lambda_0^2=\mu^2\exp\left[\frac{(4\pi v)^2}{Nm_R^2(\mu^2)}\right] . \tag{2.18}$$

The upper bound on the physical-Higgs-boson mass obtained here is in the same spirit as the lattice bound.[20,21]

Our method of solving for the pole in the scattering amplitude overlooks a pole which occurs on the negative real axis. This tachyonic pole has a mass $m_T^2=-s_0$ given by

$$m_T^2+m_R^2-Nm_T^2\frac{m_R^2}{(4\pi v)^2}\ln\left[\frac{m_T^2}{\mu^2}\right]=0 . \tag{2.19}$$

For $m_T \gg m_R$, this equation reduces to Eq. (2.18), with $m_T=\Lambda_0$. Since the scale at which the effective theory breaks down Λ is presumably less than Λ_0, we find that $m_T \gtrsim \Lambda$; i.e., the tachyon lies outside the range of validity of the effective theory.

The dashed line in Fig. 3 shows the tachyon mass m_T as a function of $m_R(\mu^2)$. Also shown, by the solid line, is the physical-Higgs-boson mass, m_H. Since $\Lambda \lesssim m_T$, the calculation of m_H is unreliable for $m_R \gg 1$ TeV, because m_H is then comparable to or greater than Λ.

In Fig. 4 we show the Higgs-boson width as a function of the physical-Higgs-boson mass (solid line). Also shown is the tree-level perturbative width (dotted line), given by

$$\Gamma_H=N\frac{m_H^3}{16\pi v^2} . \tag{2.20}$$

As m_H approaches 1 TeV, the Higgs-boson width becomes considerably broader than the tree-level estimate, attaining roughly twice the tree-level estimate for $m_H=1$ TeV. The width continues to increase as m_R is increased, in contrast with the physical mass. As $m_R \to \infty$, the width approaches twice the physical-Higgs-boson mass (indicated by the dot on the end of the solid curve).

III. THE PADÉ APPROXIMATION (REFS. 6–12)

The $[r,r]$ Padé approximation provides a means of unitarizing a perturbative expansion for an elastic scattering amplitude. Let

$$a=a_1+\cdots+a_{2r} \tag{3.1}$$

be the perturbative expansion for the Jth partial-wave amplitude to order $2r$ (the index J is suppressed). The $[r,r]$ Padé approximation is obtained by solving

$$a^{[r,r]}\equiv\frac{p_0+\cdots+p_r}{q_0+\cdots+q_r}=a_1+\cdots+a_{2r} \tag{3.2}$$

for the p_l and q_l in terms of the a_l, up to order $2r$. The resulting expression for the partial-wave amplitude satisfies the elastic two-body unitarity relation given in Eq. (2.9).

To demonstrate the procedure, let us construct the [1,1] Padé approximation to the singlet Goldstone-boson scattering amplitude. We must solve

$$a^{[1,1]}\equiv\frac{p_0+p_1}{q_0+q_1}=a_1+a_2 \tag{3.3}$$

for the p's and q's. Matching order by order in the coupling, we obtain

$$p_0=0 , \tag{3.4}$$

$$p_1=q_0a_1 , \tag{3.5}$$

$$0=q_1a_1+q_0a_2 , \tag{3.6}$$

from which we obtain the [1,1] Padé approximation

$$a^{[1,1]}=\frac{a_1}{1-a_2/a_1} . \tag{3.7}$$

In the large N limit, the lth-order amplitude is related to the tree amplitude by Eq. (2.6). Rewriting this equation in terms of zeroth partial-wave amplitudes yields

$$a_l=(a_l)^l(\bar{I}(s))^{l-1} , \tag{3.8}$$

where

$$\bar{I}\equiv 16\pi I . \tag{3.9}$$

Using Eq. (3.8) to replace a_2 in the expression for the [1,1] Padé approximation, Eq. (3.7), we obtain

$$a^{[1,1]}=\frac{a_1}{1-a_1\bar{I}(s)} , \tag{3.10}$$

which is precisely the $J=0$ partial wave of the exact large-N amplitude, Eq. (2.7). Thus the [1,1] Padé approximation to the Goldstone-boson scattering amplitude in the large-N limit reproduces the exact large-N result.

The $[r,r]$ Padé approximation to the large-N amplitude is obtained by solving Eq. (3.2) up to order $2r$. Using Eq. (3.8), we find

$$a^{[r,r]} \equiv \frac{p_0 + \cdots + p_r}{q_0 + \cdots + q_r} = \frac{a_1}{1 - a_1 \bar{I}} - \frac{(a_1)^{2r+1} \bar{I}^{2r}}{1 - a_1 \bar{I}} \ . \tag{3.11}$$

Since the second term on the right-hand side of Eq. (3.11) begins at order $2r+1$, it does not contribute when we match orders of perturbation theory up to order $2r$. The first term, which equals the exact large-N amplitude, is a ratio of polynomials and, therefore, due to the uniqueness of the Padé approximation, is the $[r,r]$ Padé approximant. Thus the $[r,r]$ Padé approximation reproduces the exact large N-amplitude for all r. The reader may wish to check this assertion by constructing the [2,2] approximant.[22]

IV. THE K MATRIX (REFS. 4–6, 9, AND 13)

The K matrix is related to the S matrix by

$$S \equiv 1 + iA = \frac{1 + (i/2)K}{1 - (i/2)K} \ , \tag{4.1}$$

which ensures the unitarity of the S matrix (for K Hermitian). Projecting out the partial-wave amplitudes, we find

$$a^K = \frac{k}{1 - ik} \ , \tag{4.2}$$

where k is the Jth partial wave of K. The partial waves of K may be calculated perturbatively by equating Eq. (4.2) to the perturbative expansion of a, expanding k perturbatively, and matching orders of perturbation theory. We find

$$k_1 = a_1 \ , \tag{4.3}$$

$$k_2 = \mathrm{Re} a_2 \ , \tag{4.4}$$

$$k_3 = \mathrm{Re} a_3 + a_1^3 \ , \tag{4.5}$$

and so forth. The resulting partial-wave amplitude, Eq. (4.2), satisfies the unitarity relation Eq. (2.9).

The tree-level K-matrix approximation to the $J=0$ singlet Goldstone-boson scattering amplitude, in the large-N limit, is

$$a_1^K = \frac{a_1}{1 - i a_1} = -\frac{N}{16\pi} \frac{m_0^2}{v^2} \frac{s}{s - m_0^2 + iNs(m_0^2/16\pi v^2)} \ . \tag{4.6}$$

To compare this amplitude with the exact large-N amplitude, Eq. (2.11), we relate the bare coupling m_0 to the scale-dependent renormalized coupling $m_R(\mu^2)$ via the tree-level relation $m_0 = m_R(\mu^2)$. We find that the tree-level K matrix does not reproduce the exact large-N amplitude for any choice of μ^2.

We may solve for the physical mass and width of the Higgs resonance in the tree-level K-matrix amplitude just as we did in the exact large-N amplitude. The solution is identical, with the exception that Eq. (2.15) is replaced by

$$\tan\theta = -N \frac{m_R^2}{(4\pi v)^2} \pi \ . \tag{4.7}$$

We show in Fig. 5 the physical-Higgs-boson mass as a function of the bare mass parameter m_0. As in the exact solution, the physical mass saturates as the coupling increases, although at a higher value, $m_H = 1147$ GeV. As $m_0 \to \infty$, the physical mass decreases slowly, approaching 1007 GeV asymptotically.

When comparing the dependence of the physical-Higgs-boson mass on the bare mass parameter in Fig. 5 with the exact result, given in Fig. 2, one must keep in mind that m_R^2 in Fig. 2 is scale dependent. We have chosen $\mu^2 = |s_0|$, but other choices could be made, which would result in a different dependence of m_H^2 on m_R^2. In particular, Refs. 5–9 use $\mu^2 = m_R^2$ which, for $m_R^2 \gg m_H^2$, is much larger than $|s_0|$.

The dependence of the Higgs-boson width on the physical-Higgs-boson mass provides a scale-independent basis for comparison of the K-matrix amplitude with the exact amplitude. The Higgs-boson width as a function of the physical-Higgs-boson mass in the tree-level K-matrix approach is given by the dashed line in Fig. 4. The K-matrix curve lies between the exact solution (solid line) and the perturbative tree approximation (dotted line). Thus, although the tree-level K matrix does not reproduce the exact large-N result, it improves upon the ordinary tree-level approximation.

To construct the lth-order K-matrix amplitude, we calculate $k = k_1 + \cdots + k_l$, perturbatively renormalize, and insert the resulting expression into Eq. (4.2). We find that the lth-order renormalized contribution to the K matrix is

$$k_l = -\frac{N}{16\pi} \frac{m_R^2}{v^2} \frac{s}{s - m_R^2} \left[N \frac{s}{s - m_R^2} \frac{m_R^2}{(4\pi v)^2} \ln \frac{|s|}{\mu^2} \right]^{l-1} \ . \tag{4.8}$$

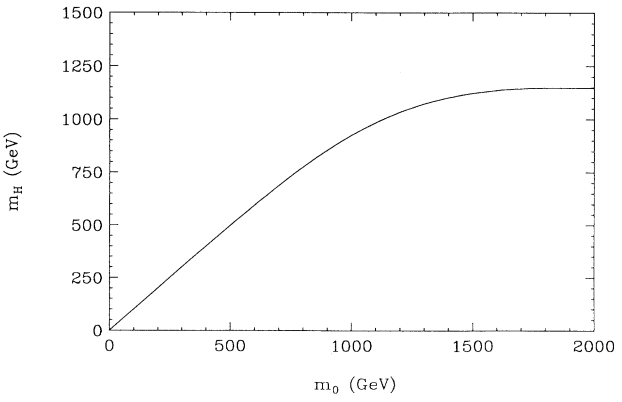

FIG. 5. The physical-Higgs-boson mass as a function of the bare mass parameter in the tree-level K-matrix approximation to the O($2N$) model for large N. The physical mass goes to 1007 GeV as $m_0 \to \infty$.

Summing to all orders, we obtain

$$k=\sum_{l=1}^{\infty} k_l = -\frac{N}{16\pi}\frac{m_R^2}{v^2}\frac{s}{s-m_R^2-Ns[m_R^2/(4\pi v)^2]\ln(|s|/\mu^2)}, \tag{4.9}$$

which yields[23]

$$a^K=-\frac{N}{16\pi}\frac{m_R^2}{v^2}\frac{s}{s-m_R^2-Ns[m_R^2/(4\pi v)^2]\ln(-s/\mu^2)} \tag{4.10}$$

which is the zeroth partial wave of the exact large N amplitude, Eq. (2.11). Thus the K-matrix approach reproduces the exact amplitude when summed to all orders, as it should. However, it differs from the exact result at any finite order.

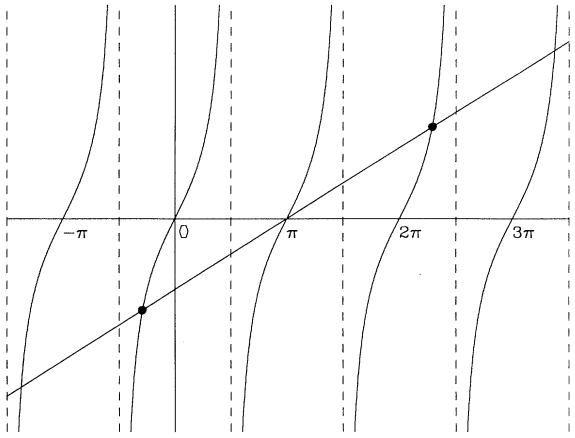

FIG. 6. Graphical representation of Eq. (2.15), where the x axis is θ. The dots indicate the position of poles in the scattering amplitude.

V. DISCUSSION

Our analysis of the O(2N) model in the large-N limit supports the contention that the Padé and K-matrix approximations improve upon ordinary perturbation theory. The $[r,r]$ Padé approximation to the Goldstone-boson scattering amplitude reproduces the exact amplitude for all r, to leading order in $1/N$. The tree-level K matrix yields an amplitude qualitatively similar to the exact large N amplitude. The K matrix does not reproduce the exact amplitude at any finite order, but it does approach the exact amplitude as the order increases.

One cannot make a conclusive statement regarding the validity of the Padé and K-matrix approximations, in general, based on our analysis. The O(2N) model in the large-N limit is a simple model, lacking a spectrum of resonances which one might expect in a strongly interacting theory. It would be interesting to apply these approximations to models with more structure.

ACKNOWLEDGMENTS

I am grateful to R. Pisarski for many conversations on the $1/N$ expansion and to F. Paige for a very helpful conversation. I have also benefited from conversations with D. Dicus, R. Longacre, Y. Shen, and G. Valencia. This manuscript has been authored under Contract No. DE-AC02-76CH00016 with the U.S. Department of Energy.

APPENDIX

In this appendix we discuss the analytic structure of the singlet Goldstone-boson scattering amplitude, Eq. (2.11). In Sec. II we solved for the poles of this amplitude, s_0, by choosing $\mu^2=|s_0|$; clearly $\mu^2\geq 0$. Writing $s_0=\mu^2 e^{i\theta}$, we obtained Eq. (2.15) and Eq. (2.16) for θ and μ^2, respectively. Equation (2.15) is shown graphically in Fig. 6; the straight line has a y intercept of $-N\pi m_R^2/(4\pi v)^2$, and its intersections with the tangent function are solutions of the equation. However, the intersection at $\theta=\pi$, as well as the intersections of the branches of the tangent function which pass through $\theta=3\pi$, 5π, . . . and $\theta=-\pi$, -3π, . . . correspond, via Eq. (2.16), to $\mu^2<0$; they therefore do not correspond to poles, since $\mu^2\geq 0$ by definition. The physical sheet corresponds to $0<\theta<2\pi$; we see that there are no poles there, as demanded by causality. The intersection in the quadrant $-\pi/2<\theta<0$ corresponds to a pole on the second Riemann sheet, below the positive real axis; we identify this with the physical Higgs particle. Also shown is a pole on the Riemann sheet above the physical sheet, in the quadrant $2\pi<\theta<5\pi/2$. There are also poles corresponding to the intersections of the branches of the tangent function which pass through $\theta=4\pi$, 6π, . . . and $\theta=-2\pi$, -4π, ...

The analytic structure of the scattering amplitude may thus be summarized as follows: an infinite set of Riemann sheets, connected by branch cuts that run from the origin to infinity at $\theta=0$, 2π, 4π, . . . and $\theta=-2\pi$, -4π, . . .; one may envision this as a helix winding around a line drawn vertically though the origin of the complex plane, with each turn of the helix corresponding to a different sheet. The sheets below the physical sheet have a pole in the quadrant below the branch cut, while the poles in the sheets above the physical sheet occur in the quadrant above the branch cut. There is no pole on the physical sheet, except a pole on the negative real axis, which corresponds to a tachyon. As we discussed in Sec. II, this pole occurs outside the range of validity of our effective-field-theory calculation.

[1]D. Dicus and V. Mathur, Phys. Rev. D **7**, 3111 (1973); B. Lee, C. Quigg, and H. Thacker, *ibid.* **16**, 1519 (1977).

[2]M. Chanowitz and M. K. Gaillard, Nucl. Phys. **B261**, 379 (1985).

[3]W. Marciano, G. Valencia, and S. Willenbrock, Phys. Rev. D **40**, 1725 (1989).

[4]W. Repko and C. Suchyta, Phys. Rev. Lett. **62**, 859 (1989).

[5]D. Dicus and W. Repko, Phys. Lett. B **228**, 503 (1989).

[6]D. Dicus and W. Repko, Phys. Rev. D **42**, 3660 (1990).

[7]A Dobado, Phys. Lett. B **237**, 457 (1990).

[8]A. Dobado, M. Herrero, and T. Truong, Phys. Lett. B **235**, 129 (1990).

[9]A. Dobado, M. Herrero, and J. Terron, Report No. CERN-TH-5670/90 (unpublished).

[10]D. Bessis and M. Pusterla, Nuovo Cimento **54A**, 243 (1968); J. Basdevant, D. Bessis, and J. Zinn-Justin, *ibid.* **60A**, 185 (1969); J. Basdevant and B. Lee, Phys. Lett. **29B**, 437 (1969).

[11]K. Jhung and R. Willey, Phys. Rev. D **9**, 3132 (1974).

[12]A. Dobado, M. Herrero, and T. Truong, Phys. Lett. B **235**, 134 (1990).

[13]M. Cini and S. Fubini, Nuovo Cimento **11**, 142 (1954).

[14]S. Coleman, R. Jackiw, and H. Politzer, Phys. Rev. D **10**, 2491 (1974); H. Schnitzer, *ibid.* **10**, 1800 (1974); R. Root, *ibid.* **10**, 3322 (1974); M. Kobayashi and T. Kugo, Prog. Theor. Phys. **54**, 1537 (1975); L. Abbott, J. Kang, and H. Schnitzer, Phys. Rev. D **13**, 2212 (1976); R. Haymaker *ibid.* **13**, 968 (1976).

[15]W. Bardeen and M. Moshe, Phys. Rev. D **28**, 1372 (1983).

[16]M. Einhorn, Nucl. Phys. **B246**, 75 (1984); see also R. Casalbuoni, D. Dominici, and R. Gatto, Phys. Lett. **147B**, 419 (1984).

[17]M. Veltman and F. Yndurain, Nucl. Phys. **B325**, 1 (1989).

[18]K. Wilson, Phys. Rev. D **6**, 419 (1972); K. Wilson and J. Kogut, Phys. Rep. **12C**, 75 (1974); G. Baker and J. Kinkaid, J. Stat. Phys. **24**, 469 (1981); B. Freeman, P. Smolensky, and D. Weingarten, Phys. Lett. **113B**, 481 (1982); J. Frohlich, Nucl. Phys. **B200**, 281 (1982); M. Aizenman, Phys. Rev. Lett. **47**, 1 (1981).

[19]The factor N arises from summing over the $(2N-1)^2$ channels, multiplying by the normalization factor $1/2(2N-1)$, and taking the large-N limit.

[20]R. Dashen and H. Neuberger, Phys. Rev. Lett. **50**, 1897 (1983); A. Hasenfratz and T. Neuhaus, Nucl. Phys. **B297**, 205 (1988); W. Langguth and I. Montvay, Z. Phys. C **36**, 725 (1987); P. Hasenfratz and J. Nager, *ibid.* **37**, 477 (1988); A. Hasenfratz, T. Neuhaus, K. Jansen, H. Yoneyama, and C. Lang, Phys. Lett. B **199**, 531 (1987); J. Kuti, L. Lin, and Y. Shen, Phys. Rev. Lett. **61**, 678 (1988); M. Luscher and P. Weisz, Phys. Lett. B **212**, 472 (1988).

[21]M. Einhorn and D. Williams, Phys. Lett. B **211**, 457 (1988).

[22]Should the reader accept this invitation, he/she will encounter a degenerate system of equations. This degeneracy is cancelled when forming the Padé approximant, however. The $[r,r]$ Padé approximation procedures an $r-1$ degenerate system of equations.

[23]We remove the absolute value signs from the argument of the logarithm to analytically continue the amplitude into the complex plane.